2012 NDIA GROUND VEHICLE SYSTEMS ENGINEERING AND TECHNOLOGY SYMPOSIUM
MODELING & SIMULATION, TESTING AND VALIDATION (MSTV) MINI-SYMPOSIUM
AUGUST 14-16, MICHIGAN

PERFORMANCE RESULTS FOR A UNIVERSAL LITHIUM ION BATTERY MANAGEMENT SYSTEM

Bruce Pilvelait
Carlos H. Rentel
William Finger
Larry Ruckman
David Fogg
Creare Incorporated
Hanover, NH

Gregory L. Plett
University of Colorado
Colorado Springs, CO

Mike Marcel
A123 Systems
Livonia, MI

ABSTRACT

The advantages of lithium-based batteries over lead acid batteries have created great interest in developing safe and cost effective drop-in replacements. To achieve the required cost effectiveness and safety of the battery, Battery Management Systems (BMS) are critical to avoid over-charging, over-discharging, and continuously and accurately determining the State of Charge (SOC), State of Health (SOH), and State of Life (SOL) of the battery. In a program funded through a U.S. Army–TARDEC SBIR, the authors developed and tested a military-grade BMS that includes: (1) a Kalman Filter-based SOC estimation algorithm with better than 5% accuracy; (2) continuous cell monitoring to avoid over-charging or over-discharging; (3) active and passive cell balancing; (4) an innovative, low cost, and high-accuracy current sensing method; and (5) vehicle-level communication capability. Our BMS uses a modular, universal architecture that supports any lithium-based chemistry, pack size, or configuration. This is particularly important when multiple packs are series connected to achieve high voltage. This paper presents our design approach, test data which validate performance expectations, and our plans for integrating this BMS with an emerging class of 6T format batteries for U.S. Army tactical vehicle starting and Silent Watch energy storage needs.

INTRODUCTION

Lithium-based batteries promise excellent performance in terms of lifetime, energy density, and power density. However, they require careful management to avoid personnel injury and equipment damage. Consequently, there is extreme interest in developing an accurate Battery Management System (BMS) to take advantage of the positive attributes of lithium-based chemistries without sacrificing flexibility and safety. However, the lack of proper BMS standardization and inaccurate state estimation algorithms has hampered the widespread adoption of lithium chemistries in spite of their advantages. In this paper we describe our BMS and present results that show that we can: (1) provide State of Charge (SOC) estimation accuracy to better than 5%; (2) provide a universal architecture that is adaptable to other chemistries, capacities and formats; (3) actively balance the series cells in a pack; and (4) enable operation over a wide range of temperatures. The primary application that we

Report Documentation Page

Form Approved
OMB No. 0704-0188

Public reporting burden for the collection of information is estimated to average 1 hour per response, including the time for reviewing instructions, searching existing data sources, gathering and maintaining the data needed, and completing and reviewing the collection of information. Send comments regarding this burden estimate or any other aspect of this collection of information, including suggestions for reducing this burden, to Washington Headquarters Services, Directorate for Information Operations and Reports, 1215 Jefferson Davis Highway, Suite 1204, Arlington VA 22202-4302. Respondents should be aware that notwithstanding any other provision of law, no person shall be subject to a penalty for failing to comply with a collection of information if it does not display a currently valid OMB control number.

1. REPORT DATE	2. REPORT TYPE	3. DATES COVERED
12 AUG 2012	**Journal Article**	**12-08-2012 to 12-08-2012**

4. TITLE AND SUBTITLE
PERFORMANCE RESULTS FOR A UNIVERSAL LITHIUM ION BATTERY MANAGEMENT SYSTEM

5a. CONTRACT NUMBER
W56HZV-11-C-0194

5b. GRANT NUMBER

5c. PROGRAM ELEMENT NUMBER

6. AUTHOR(S)
Bruce Pilvelait; Gregory Plett; Mike Marcel; Carlos Rentel; William Finger

5d. PROJECT NUMBER

5e. TASK NUMBER

5f. WORK UNIT NUMBER

7. PERFORMING ORGANIZATION NAME(S) AND ADDRESS(ES)
A123 Systems,39000 Seven Mile Rd.,Livonia,MI,48152

8. PERFORMING ORGANIZATION REPORT NUMBER
; #23142

9. SPONSORING/MONITORING AGENCY NAME(S) AND ADDRESS(ES)
U.S. Army TARDEC, 6501 E.11 Mile Rd, Warren, MI, 48397-5000

10. SPONSOR/MONITOR'S ACRONYM(S)
TARDEC

11. SPONSOR/MONITOR'S REPORT NUMBER(S)
#23142

12. DISTRIBUTION/AVAILABILITY STATEMENT
Approved for public release; distribution unlimited

13. SUPPLEMENTARY NOTES
Submitted to 2012 NDIA GROUND VEHICLE SYSTEMS ENGINEERING AND TECHNOLOGY SYMPOSIUM August 14-16, Michigan

14. ABSTRACT

The advantages of lithium-based batteries over lead acid batteries have created great interest in developing safe and cost effective drop-in replacements. To achieve the required cost effectiveness and safety of the battery, Battery Management Systems (BMS) are critical to avoid over-charging, over-discharging, and continuously and accurately determining the State of Charge (SOC), State of Health (SOH), and State of Life (SOL) of the battery. In a program funded through a U.S. Army?TARDEC SBIR, the authors developed and tested a military-grade BMS that includes: (1) a Kalman Filter-based SOC estimation algorithm with better than 5% accuracy; (2) continuous cell monitoring to avoid over-charging or over-discharging; (3) active and passive cell balancing; (4) an innovative, low cost, and high-accuracy current sensing method; and (5) vehicle-level communication capability. Our BMS uses a modular, universal architecture that supports any lithium-based chemistry, pack size, or configuration. This is particularly important when multiple packs are series connected to achieve high voltage. This paper presents our design approach, test data which validate performance expectations, and our plans for integrating this BMS with an emerging class of 6T format batteries for U.S. Army tactical vehicle starting and Silent Watch energy storage needs.

15. SUBJECT TERMS

16. SECURITY CLASSIFICATION OF:			17. LIMITATION OF ABSTRACT	18. NUMBER OF PAGES	19a. NAME OF RESPONSIBLE PERSON
a. REPORT **unclassified**	b. ABSTRACT **unclassified**	c. THIS PAGE **unclassified**	**Same as Report (SAR)**	**11**	

Standard Form 298 (Rev. 8-98)
Prescribed by ANSI Std Z39-18

describe is for Silent Watch, but the BMS and these algorithms are also suitable for Electric Vehicle (EV) and Hybrid Electric Vehicle (HEV) applications. Our BMS will enable the future of lithium-ion batteries through the safe and flexible incorporation of the latest battery packs.

SYSTEM DESCRIPTION

Figure 1 illustrates our concept for a BMS that provides health monitoring for a typical 24 VDC Silent Watch pack [1]. In most lithium-based battery pack applications, the pack is comprised of a number of series- and parallel-connected cells to achieve the required voltage, current, and energy/power capacity. As one example, a typical Silent Watch configuration could consist of eight sub-modules of six parallel-connected, prismatic, 3.3 V, 20 Ah cells (8S6P). In total, there are 48 cells in this configuration, the nominal pack voltage is 26.4 V, and the capacity is 120 Ah. The parallel-connected cells are referred to as "super-cells" and require relatively little oversight compared to the series-connected cells, which pose the most challenges because of the need for cell balancing. The BMS monitors the voltage and temperature of each super-cell and the series current of the overall pack via individual super-cell sense modules. Although this particular Silent Watch battery pack uses eight series-connected super-cells, this Universal BMS architecture is expandable to any number of super-cells, extending support from Silent Watch to that of HEV power packs, for example. The Master Central Unit, implemented with a digital signal processor (DSP), provides control and reporting functions and manages charge cycle and balancing for each individual super-cell, thereby ensuring safety and highly competitive performance. The DSP also uses SOC/SOL/SOH, power availability, and thermal monitoring algorithms to optimize and report on cell performance. Finally, a communication interface using a Controller Area Network (CAN) is implemented to link the BMS associated with a single pack module to a larger system, such as to the vehicle monitoring/ controlling system, and to other BMSs associated with other pack modules. Figure 2 shows the core electronic assembly that implements most of the functionality shown in Figure 1. Pack protection and current switching hardware is implemented in a different module that interfaces to this module.

We have created a system that can be integrated with a Lithium-based battery pack in a 6T form factor. This is illustrated in the mechanical model of Figure 3, where the electronic assembly in Figure 2 is located on the top of the battery pack. Our BMS effectively transforms a battery pack into an intelligent module capable of detail battery state reporting, protection, extensibility, and managing functionality into a single package. The latter has the goal of maximizing the performance benefits of Lithium-based packs while ensuring safety.

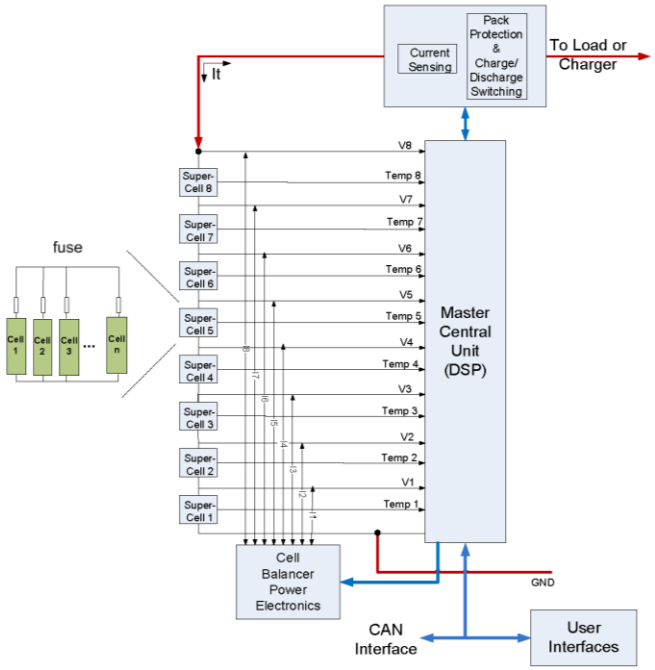

Figure 1. BMS architecture for a 24 VDC lithium-ion based Silent Watch battery pack capable of SOC, SOH, SOL, power availability, thermal monitoring, protection, and active cell balancing

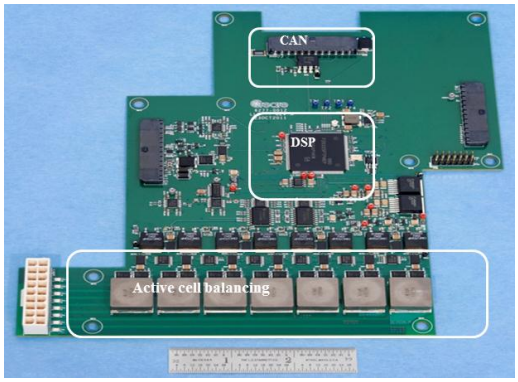

Figure 2. Core BMS electronics implementing the master central unit, communications, active cell balancing, and voltage, current, and temperature monitoring and signal conditioning.

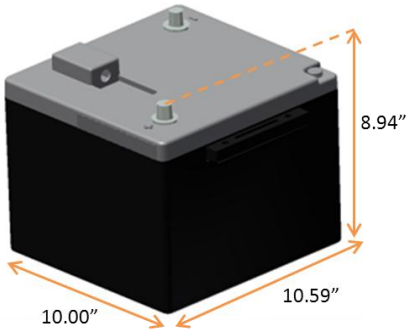

Figure 3. 24VDC 6T pack dimensions with A123 Systems' lithium nano-phosphate prismatic cells.

Battery Pack and BMS Protective and Health Monitoring Elements

The BMS includes a number of battery pack and BMS protective and health monitoring capabilities. These protection features include pack and cell over-voltage, under-voltage, overcurrent, and over-temperature monitoring. The BMS operates in two user-selectable modes within the context of protection and health monitoring functionality: a normal protection mode, and a battle-override protection mode. In the normal mode the BMS maintains the pack within limits designed to ensure a longer battery life and the safety of systems and entities interfacing with it (e.g., personnel, electric loads, and chargers).

In the battle override mode, the BMS is exclusively concerned with personnel safety rather than the long-term health and life of the battery. As a consequence, the normal mode has more stringent battery protection limits than the battle override mode. The primary overcurrent protection feature is realized in hardware by Solid State Circuit Breakers (SSCB) developed with a set of parallel N-Type MOSFETs. These circuit breakers can allow and control current in both directions (to force a charge-only, discharge-only, or charge-discharge current direction into or out of the pack). Additionally, the current sensing capability is embedded into these units by leveraging the MOSFETs' drain-source resistance as a current shunt sensor, which is calibrated at different temperatures.

Currently, a user can interface to our BMS via a Personal Computer (PC). The PC runs a CAN application that shows cell voltages, SOC, temperatures, error/diagnostic messages, and current in tabular or graphical screens. It is also possible to control and configure the BMS via this application. For instance, cell balancing can be enabled or disabled, and the user can select between battery override and normal protection mode. Figure 4 shows typical screens in our BMS user interface.

SILENT WATCH REQUIREMENTS

This BMS aims to benefit a new breed of lithium-based battery packs currently being developed. Reference [1] shows one example. The energy for Silent Watch applications is currently provided by two series-connected lead acid batteries, such as the ArmaSafe 6T, 12 VDC, 120 Ah battery. Silent Watch energy needs range from an average power requirement of 1.5 kW for 2 to 6 hours to a short-term peak power requirement of almost 5 kW according to [1]. There are two most obvious ways to achieve this goal using standard format lithium-ion cells that we know are of interest for Silent Watch applications. These include the 26650 cylindrical cells and the prismatic cell.

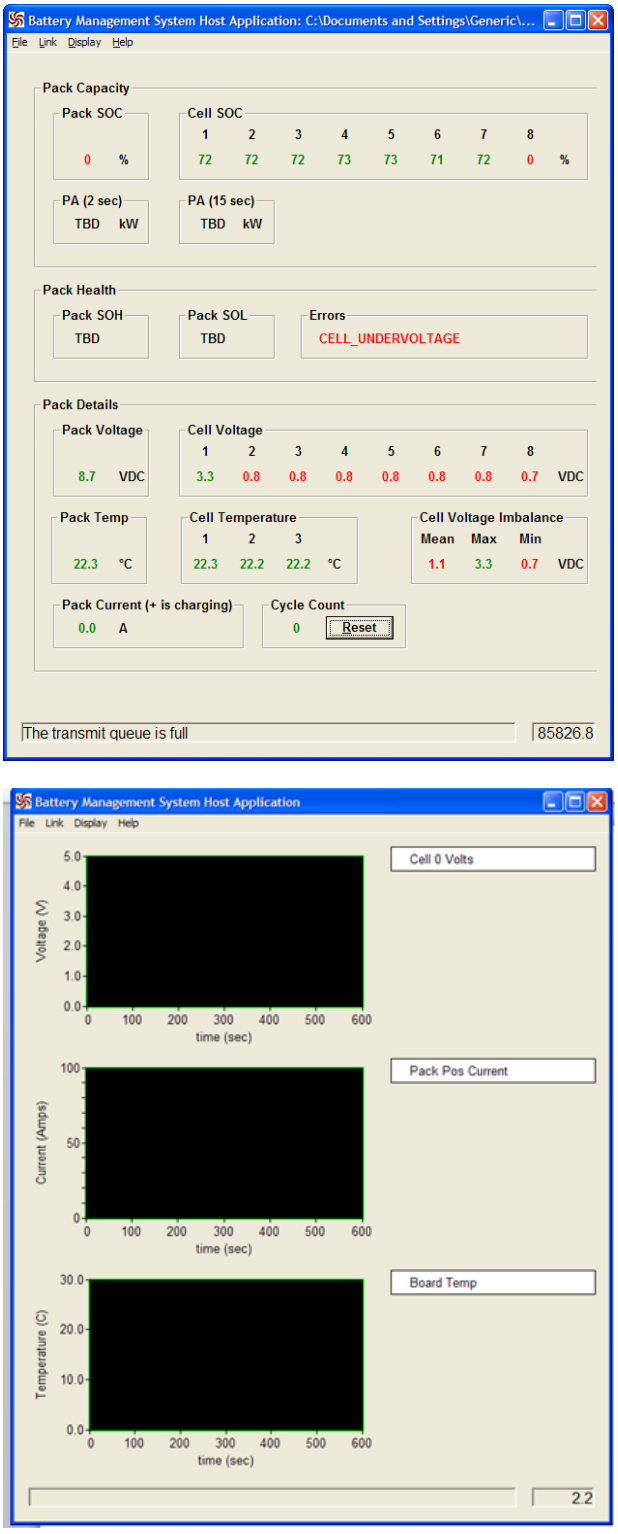

Figure 4. BMS graphical user interface using the CAN bus

Figure 5a shows the configuration of 8 sub-modules (also referred to as super-cells in Figure 1) of 52 parallel-connected A123 26650, 3.3 V, 2.3 Ah cells (8S52P). In total, there are 416 cells, the nominal pack voltage is 26.4 V, and the capacity is 120 Ah. Figure 5b shows the configuration of 8 sub-modules of 6 parallel-connected A123 prismatic, 3.3 V, 20 Ah cells (8S6P). In total, there are 48 cells, the nominal pack voltage is 26.4 V, and the capacity is 120 Ah. Some important additional considerations in a battery pack design are the cost, power density, energy density, and volume of the packaging, which depend on the specific requirements of the application.

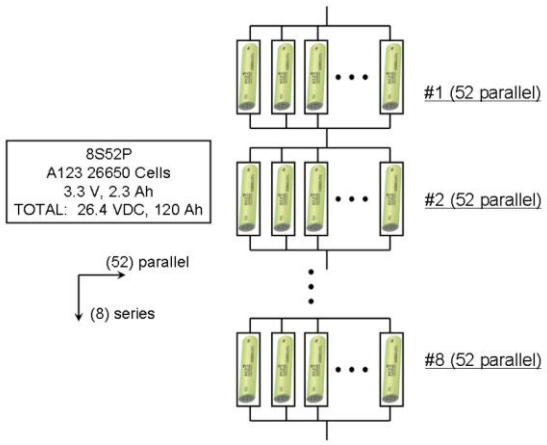

Figure 5a. 24 VDC lithium-ion pack based on 26650 type cylindrical cells (8S52P)

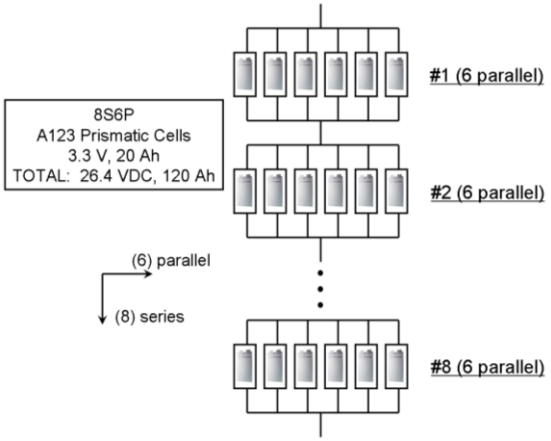

Figure 5b. 24 VDC lithium-ion pack based on prismatic lithium cells (8S6P)

In both cases, an effective method for configuring a BMS is to provide voltage, temperature, SOC, SOL, SOH estimation, and cell balancing at the sub-module level. This method ensures a minimal number of sensing points and hardware size, while still achieving the main goal of providing accurate pack monitoring. However, cell level electrical protection and temperature monitoring may still be needed at some level to guarantee maximum safety. For more details of the Silent Watch requirements, refer to [1] and [2].

In a previous paper we described the SOC algorithm and test results using laboratory equipment and cylindrical 26650 cells [2]. Those results helped us validate the accuracy of the SOC algorithm prior to the development of the BMS prototype. In this paper we present a summary of the results obtained in two major tasks we have completed recently: (1) the modeling of the A123 prismatic 20Ah cells, and (2) the implementation and testing of the first generation prototype BMS. In the following two sections, we present cell level laboratory test results and BMS integrated hardware test results.

CELL MODELING LABORATORY TEST RESULTS

Prismatic cells have a substantial packaging advantage over cylindrical cells. For a given volume, and due to geometrical reasons, a pack formed with prismatic cells can have a larger energy and power density than a pack formed with cylindrical cells. Additionally, depending on the manufacturer, prismatic cells may have different electrical performance, and therefore they represent an important alternative to cylindrical cells. In this task we modeled the 20Ah prismatic cells from A123 Systems. An important outcome of this model is that it essentially maintains the same structure as the one used for cylindrical cells [2], and previous model results in [3], [4], and [5] with only different parameter values. This implies that, consistent with our goal of developing a BMS which can be universally applied to any lithium-ion battery pack, our BMS is capable of operating with both cylindrical and prismatic cells after a simple software update. For instance, a user will be able to choose from a library of battery chemistries the one that matches the chemistry of its pack, then update the software and expect the BMS to manage the pack immediately.

Test Facility Description

We have made use of the 540-square-foot High-Capacity Battery Research and Test Laboratory of the University of Colorado at Colorado Springs for this task [8]. The laboratory has facilities to perform automated tests on high-capacity cells (such as might be used in EVs and HEVs), modules of such cells, and full-sized battery packs. The laboratory has several battery cyclers capable of handling powers up to 170 kW and thermal chambers.

Test Results

Figure 6 shows the SOC comparison results of our model at several different cell ambient temperatures, ranging from -30°C up to +55°C and using a Silent Watch Load profile based on [1] and [2].

We use a Precise Coulomb count as a benchmark for true SOC ("True" SOC green curve in Figure 6). This benchmark is deemed valid because we are utilizing highly precise state-of-the-art current and voltage measurement equipment (unsuitable for field deployment due to cost and size), and because the load profile is run only for a short period of time, both of which imply that errors are small and are not accumulated substantially in these tests. The "true" SOC results shown in Figure 6 are quite accurate, so the desire is for the SOC algorithm estimate ("SPKF SOC") to agree to validate its accuracy. As shown in Figure 6, the algorithm does quite well for temperatures between -30°C and +55°C.

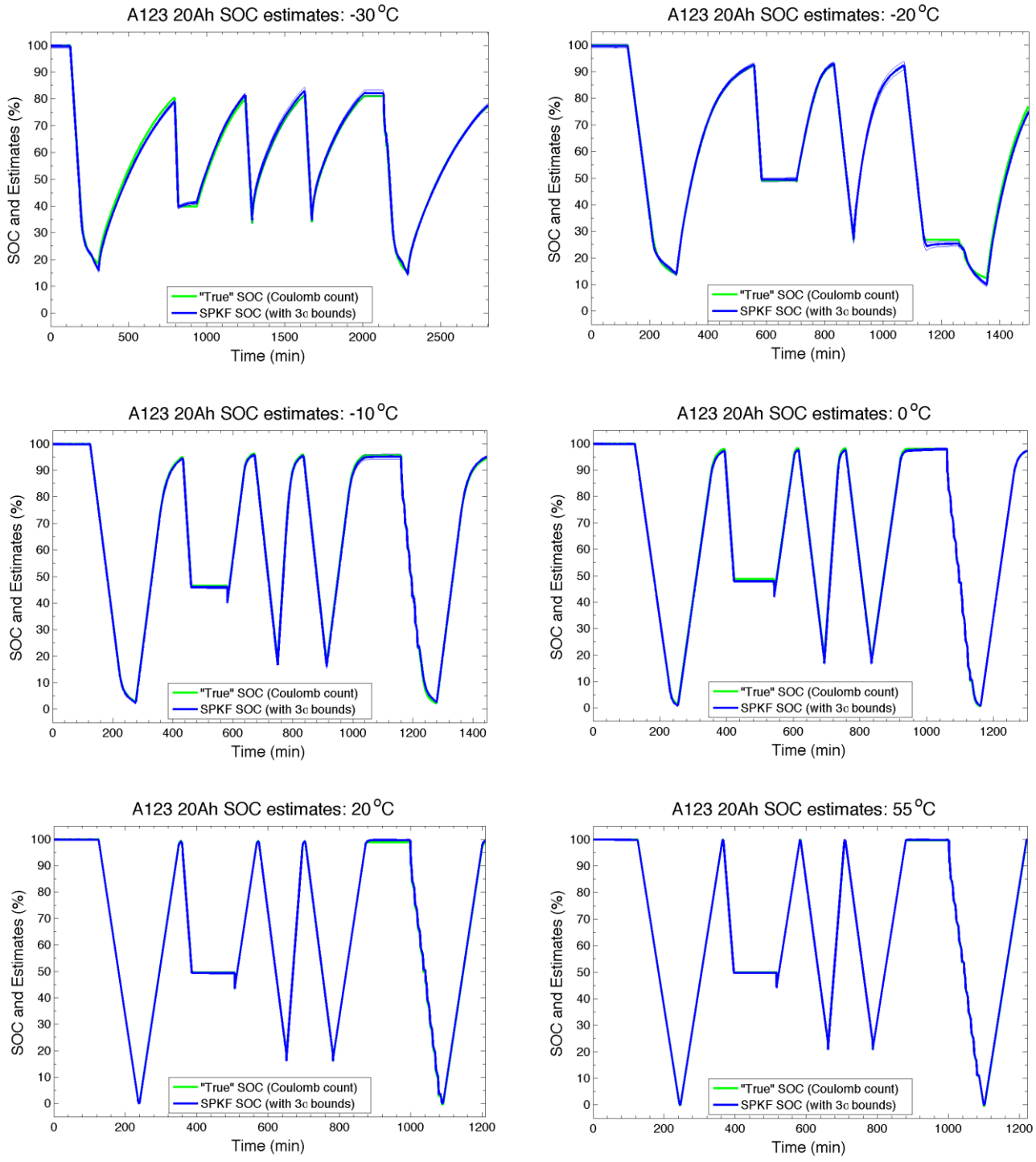

Figure 6. SOC comparison tests for -30°C up to +55°C

The results shown in Figure 6 correspond to tests performed with a single prismatic cell. These results may vary for different cells due to structural differences caused by manufacturing variability. We performed the same tests with three different cells and indeed obtained different results. An analysis of these results reveals that the average error across time is within 3% for all temperatures tested. To better quantify SOC estimation accuracy, we took all the SOC results and computed the mean and standard deviation of the error over time (over a single discharge or a single charge time frame). The mean and standard deviation of these errors are shown in Figure 7 for a temperature range between -30°C and +55°C. As shown, mean error remains less than 2%. SOC error can momentarily move away from the 3% threshold, with a worst case standard deviation of the error of roughly 6% at -30°C. For example, at the coldest temperatures, at rapidly changing SOC, and when the algorithm has not had an opportunity to compensate for detected errors, the error may temporarily be large relative to other times. However, over time, the algorithm is able to compensate and correct for detected errors and the mean error remains less than 2%. We believe this is an excellent result considering the behavior of any state-of-the-art cell will be somewhat erratic at extreme low temperatures.

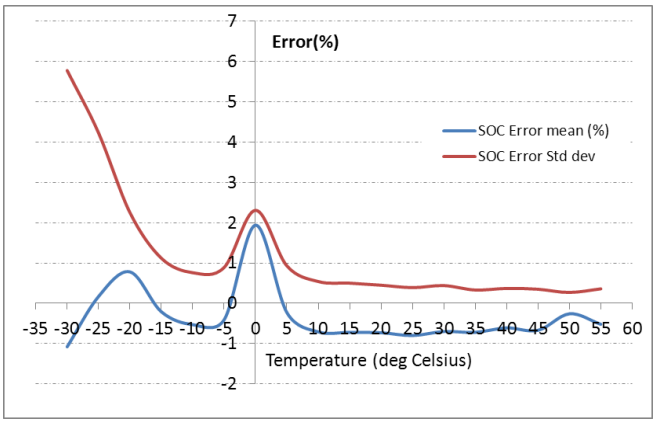

Figure 7. Average SOC error for the prismatic 20Ah cell model

For details of the model and algorithm used, see [6] and [7]. Next we present results of our tests with our first BMS integrated hardware prototype.

BMS PROTOTYPE TEST RESULTS

We have fabricated a first generation prototype BMS to implement these algorithms. The prototype implements the system illustrated in Figure 1, including voltage, current, temperature sensing/monitoring, pack and cell protection features, inductive-based active cell balancing, passive cell balancing, SOC algorithm, CAN communication interface, and PC application for user interface. Additionally, our hardware prototype has been designed to operate in a military temperature range of -55°C up to +70°C. We used an 8S1P pack comprised of eight A123 26650 cells in series. That is a pack with nominal voltage of 26.4VDC and 2.5Ah capacity. In what follows we present and describe the most important test results with this prototype and battery pack.

Voltage and Temperature Measurements

The most fundamental function of the BMS is to accurately measure voltages, temperatures, and current. All these variables are used as inputs for the protection functions and battery pack algorithms. An error in these measurements immediately escalates into algorithm errors and malfunctioning of the BMS. Voltage and temperature are relatively straightforward variables to measure, and for brevity it suffices to say that voltage and temperature measurement errors, across a cell output voltage range of 1VDC up to 4VDC, and temperatures from -55°C to +70°C, are well within 1%. The voltage results were obtained by comparing to precision digital multi-meters, and the different temperatures were obtained by placing the BMS into a thermal chamber for a period of at least 2 hrs for each temperature of interest in the aforementioned temperature range. We use NTCs for temperature measurements.

Current Measurement

Accurate current measurement is both critical and challenging. The SOC, SOH, and SOL algorithm accuracy depends considerably on the accuracy of current measurement. Additionally, the combination of physical space constraints (see Figure 3), power handling and temperature range requirements (i.e., -55°C up to +70°C) make it difficult to use classical current sensing techniques, such as shunts or Hall-effect sensors. We are able to circumvent this problem by measuring current without adding extra sensors. In particular, the Solid-State Circuit Breakers (SSCB) are comprised of a number of MOSFETs in parallel. When a MOSFET is switched ON, it behaves as a small resistor between its drain and source terminals. This resistance is referred to as the drain-to-source on-state resistance ($R_{ds\text{-}on}$) and is very well behaved, though difficult to measure because it is so low. Using very carefully designed instrumentation for the BMS, we use the voltage across the $R_{ds\text{-}on}$ of one of the SSCBs to infer the current in and out of the pack. The $R_{ds\text{-}on}$ in every MOSFET is dependent on the MOSFET batch and the junction temperature. Therefore, a temperature compensated current calibration procedure is required for this method. To accomplish this compensation, we performed current calibration and obtained a current to $R_{ds\text{-}on}$ voltage (amp/volt) relationship at different temperatures. Figure 8 shows the error of the MOSFET-based current sensor as a function of current and temperature.

The maximum error over the temperature range tested is < 4.5% of the full-scale range of 18A (-8A to +10A). The latter current range was chosen to respect safety limits of the 8S1P pack. The result is obtained after soaking the entire BMS, including the MOSFET SSCB, at a given temperature in the temperature chamber and passing current in both charging and discharging directions. Note that the results show comparable accuracy performance well within performance bounds of commercial current sensor products such as current shunts and Hall effect devices, which are typically on the order of 1–5% accurate.

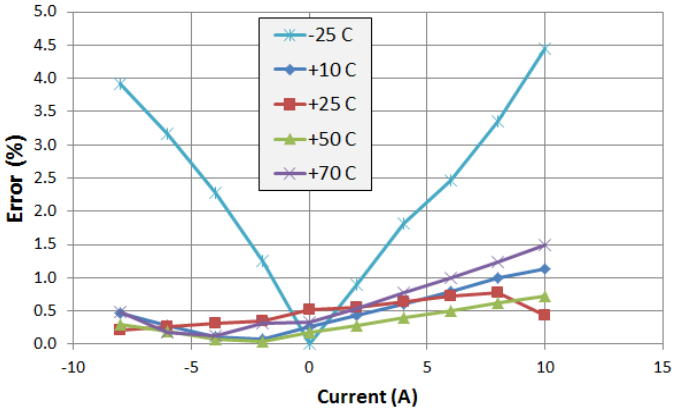

Figure 8. Error (%) of the MOSFET SSCB current sensor as a function of current and temperature. Positive current is current into the pack and out of the BMS.

While there is still ongoing work to improve the current measurement accuracy at cold temperatures and high currents, our adaptive algorithm is able to error correct to provide excellent SOC estimation results. It is important to note that the most beneficial feature of the adaptive Kalman filters is that they are able to correct small deviations based on other measurements, such as voltage and temperature, which makes our SOC algorithm robust to small current measurement errors such as these.

SOC Measurement

The prototype BMS is capable of estimating the SOC of every cell in the pack connected to it. For our tests we used an 8S1P comprised of eight A123 Systems 26650 cylindrical cells. Therefore, the model implemented in the software of the BMS corresponds to the 26650 prismatic cells (our near-term goal is to also test the BMS with prismatic cells). Due to varying cell characteristics over temperature, we are most interested in testing the accuracy of our SOC algorithm at different pack temperatures. We used a simple 2A discharge profile starting from a pack that fully charged to within 10–20%, and placed the pack and the BMS in a thermal chamber. As for the results shown in Figure 6, we used a precise

current measurement device to establish the true SOC, and compared that measurement with the SOC estimated by the prototype BMS, which uses the MOSFET SSCB current sensing method. We let the pack rest before starting the test to initialize the SOC of the pack based on the cells terminal voltages (i.e., we read the voltage and obtained the initial SOC from the Open Circuit Voltage versus SOC curve). Figures 9 through 11 show the results for -10°C, +25°C, and +45°C, respectively.

Figures 9 through 11 show the average terminal voltage of the cells versus the depth of discharge (i.e., 1-SOC) in a single discharge event. Besides the True SOC based on a Coulomb counter (using the precise current measuring equipment) as shown by the red curves, we also computed SOC using a simple Coulomb counter approach using the current measured by the MOSFET SSCB approach. The latter is referred to as BMS Current Coulomb count, and it is shown as a blue curve in the figures. The latter would be the result obtained if we would only use a Coulomb counter as our SOC algorithm instead of the more robust Kalman filter approach. It is important to note that in all these results the BMS Algorithm SOC using the Kalman filter approach (green curve) tends to approach the true SOC curve quite well.

This is in contrast to the simple approach of using the current as measured by the MOSFET SSCB alone in a simple, open loop Coulomb counter approach. This is especially true for the cold temperature (Figure 9) and high depth of discharge (70–80% DOD), although even the BMS Current Coulomb Count method is within 5–10% of the True SOC estimate in that case.

This result shows that both methods work fairly well in this tightly controlled laboratory condition of constant temperature, constant discharge current, and single discharge cycle. However, we expect that the adaptive algorithm will perform better than a Coulomb counter and will be more resilient to errors in the sensors.

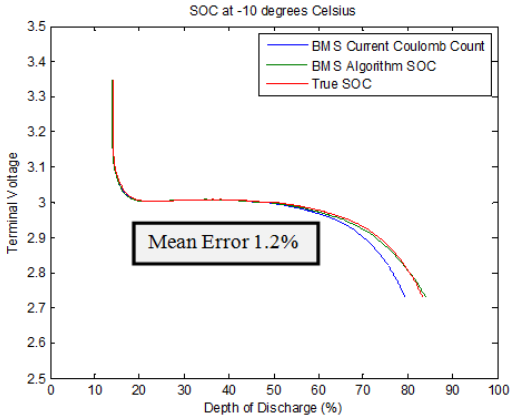

Figure 9. SOC measurements using the BMS prototype and pack at -10°C

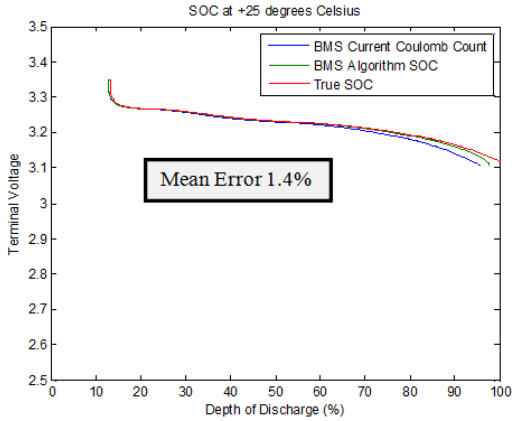

Figure 10. SOC measurements using the BMS prototype and pack at +25°C

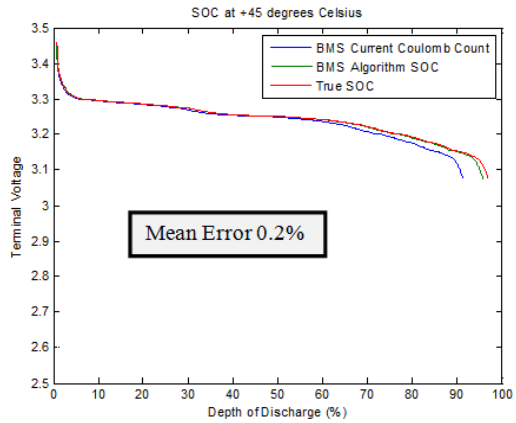

Figure 11. SOC measurements using the BMS prototype and pack at +45°C

The BMS SOC algorithm considers multiple inputs when estimating SOC, including terminal voltage, temperature, and current, which makes it more robust to measurement noises or inaccuracies than a Coulomb counter, which depends exclusively on current measurement. Our SOC algorithm computes the difference between the estimated and measured terminal voltage of every cell in the pack, and adjusts the model parameters based on temperature. Further assisting accuracy, voltage, and temperature are particularly helpful and critical at points where a cell SOC is low. At low SOC values, the voltage of the cell conveys more information about its SOC than current. All these factors make our BMS algorithm robust and accurate. The mean SOC error across the discharged time was 1.2%, 1.4%, and 0.2% for the -10°C, +25°C, and +45°C tests, respectively (the error is computed as BMS algorithm SOC minus True SOC).

Active Cell Balancing

Active cell balancing has also been implemented in the prototype hardware. It is based on the transfer of cell charge using an inductor as the intermediate energy storage device. We use a relatively simple algorithm based on cell status to determine if charge needs to be transferred and when to stop. Figure 12 shows a laboratory test of the active cell balancing algorithm on the 8S1P pack. Initially, the maximum voltage difference between the cells is approximately 70 mV. After some period of time, the active cell balancing approach brings the voltages closer to within the desired value. This result shows the convergence and proper functionality of the active cell balancing approach used in our BMS over a long period of time. The speed of the voltage convergence can be increased by adjusting control parameters and/or the inductors. It is likely that the voltage in the cells of a production-ready BMS and pack will differ by substantially less than what Figure 12 shows. Figure 12 exaggerates the initial cell voltage difference in order to test the active cell balancing circuit for a long period of time. Some cells are at 40% SOC and others are at close to 100% SOC, which is reflected in their terminal voltage at the beginning of the test. This is unlikely to happen in practice, and a faster and hence larger and more expensive active cell balancing circuit may not be necessary.

CONCLUSION

In this paper we have summarized the performance results of a Universal BMS suitable for managing lithium-based battery packs. Features of this BMS include voltage and temperature sensing, non-intrusive and accurate current sensing, accurate SOC estimation, capability to handle multiple chemistries within the lithium-ion family, active cell balancing, a complete suite of protection features, and CAN communication capability. Additionally, the BMS has been developed to operate over the full military temperature range (-55°C up to +70°C).

Tests performed with the BMS prototype have demonstrated SOC algorithm accuracies to within 2% error, and the proper functionality of active cell balancing, measurement sub-systems, and protection mechanism at different ambient temperatures.

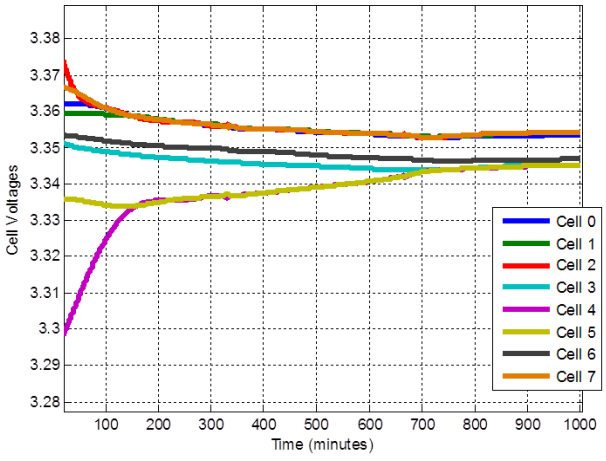

Figure 12. Pack cell voltage dynamics under active cell balancing

Our near-term goal is to test this BMS with a 26.4VDC 60Ah pack comprised of 24 20Ah prismatic cells and conforming to the 8S3P package shown in Figure 3. Additionally, we will implement the SOH, SOL, and power availability algorithms.

ACKNOWLEDGMENT

The support and guidance of the U.S. Army SBIR Office and the TACOM Research, Development and Engineering Center (TARDEC), in particular the Technical Monitor David Skalny and his team, is gratefully acknowledged. Additional support from the University of Colorado at Colorado Springs, A123 Systems and DRS-TEM is also appreciated.

REFERENCES

[1] Z. Filipi, L. Louca, A. Stefanopoulou, J. Pukrushpan, B. Kittirungsi, and H. Peng, "Fuel Cell APU for Silent Watch and Mild Electrification of a Medium Tactical Truck," Automotive Research Center, University of Michigan, SAE Paper 2004-01-1477, 2004.

[2] B. Pilvelait, C. H. Rentel, G. Plett, M. Marcel, and D. Carmen, "An Advanced Battery Management System for Lithium Ion Batteries," *National Defense Industrial Association (NDIA) Ground Vehicle Systems Engineering and Technology Symposium*, Dearborn, MI, Aug 2011.

[3] G. Plett, "Extended Kalman Filtering for Battery Management Systems of LiPB-Based HEV Battery Packs—Part 1: Background," *J. Power Sources*, Vol. 134(2), Aug 2004, pp. 252-61.

[4] G. Plett, "Extended Kalman Filtering for Battery Management Systems of LiPB-Based HEV Battery Packs—Part 2: Modeling and Identification," *J. Power Sources*, Vol. 134(2), Aug 2004, pp. 262-76.

[5] G. Plett, "Extended Kalman Filtering for Battery Management Systems of LiPB-Based HEV Battery Packs—Part 3: State and Parameter Estimation," *J. Power Sources*, Vol. 134(2), Aug 2004, pp. 277-92.

[6] G. Plett, "Sigma-Point Kalman Filters for Battery Management Systems of LiPB-Based HEV Battery Packs—Part 1: Introduction and State Estimation," *J. Power Sources*, Vol. 161(2), Oct 2006, pp. 1356–68.

[7] G. Plett, "Sigma-Point Kalman Filters for Battery Management Systems of LiPB-Based HEV Battery Packs—Part 2: Simultaneous State and Parameter Estimation," *J. Power Sources*, Vol. 161(2), Oct 2006, pp. 1369–84.

[8] High Capacity Battery Research and Test Laboratory, <http://mocha-java.uccs.edu/ HCBRTL/>, last accessed 11 July 2012.